

Theoretical Investigation of the Kinetics for the Reactions of Atomic Hydrogen with $\text{GeH}_{(4-n)}\text{Cl}_n$ ($n = 0, 1, 2, 3$)

Qingzhu Zhang, Yueshu Gu,* and Shaokun Wang

School of Chemistry and Chemical Engineering, Shandong University,
Jinan 250100, People's Republic of China

Received: September 20, 2002; In Final Form: January 24, 2003

The reactions of H atoms with GeH_4 , GeH_3Cl , GeH_2Cl_2 , and GeHCl_3 have been studied systematically using ab initio molecular orbital theory. Theoretical analysis provides conclusive evidence that the main process occurring in each case is hydrogen abstraction from the Ge–H bonds. The reaction thermal rate constants for the temperature range 200–3000 K are deduced by canonical variational transition state theory (CVT) with small curvature tunneling (SCT) correction method. The CVT/SCT rate constants exhibit typical non-Arrhenius behavior. Three-parameter rate–temperature formulas have been fitted as follows: $k_1 = 3.09 \times 10^{-17} T^{2.16} \exp(-286.74/T)$, $k_2 = 1.94 \times 10^{-17} T^{2.18} \exp(-276.82/T)$, $k_3 = 4.19 \times 10^{-18} T^{2.37} \exp(-227.64/T)$, and $k_4 = 2.02 \times 10^{-17} T^{1.98} \exp(-218.51/T)$ for the reactions of H with GeH_4 , GeH_3Cl , GeH_2Cl_2 , and GeHCl_3 , respectively (in units of $\text{cm}^3 \text{ molecule}^{-1} \text{ s}^{-1}$). Studies show that chlorine substitution has a very slight effect on the strength and reactivity of the Ge–H bonds in $\text{GeH}_{(4-n)}\text{Cl}_n$ ($n = 1-3$).

1. Introduction

Silanes and germanes are important reactants in chemical vapor deposition (CVD) used in the semiconductor industry.^{1–4} The reactions with atomic hydrogen, the simplest free-radical species, are of particular interest since these reactions provide an uncomplicated probe of chemical reactivity. In four previous contributions from this laboratory we presented the kinetic properties and theoretical rate constants for the reactions of H with fluorosilanes,⁵ chlorosilanes,⁶ methylgermanes,⁷ and fluorogermanes.⁸ As part of our ongoing work in this field, this paper investigates theoretically the kinetic properties of the reactions of H with GeH_4 , GeH_3Cl , GeH_2Cl_2 , and GeHCl_3 .

For the reaction of H with GeH_4 , several experimental studies have been reported. Two early works performed by Choo et al.⁹ and Austin et al.¹⁰ produced conflicting results. In an attempt to adjudicate between them, and to extend measurements to other temperatures, Nava et al.¹¹ and Arthur et al.¹² studied this reaction successively, and they obtained satisfactory agreement. Arthur measured the rate constants in the temperature range of 293–473 K, and combined his results with those of Nava to give a best value for rate constants of $k = (1.21 \pm 0.10) \times 10^{-10} \exp(-1008 \pm 25)/T$ (in $\text{cm}^3 \text{ molecule}^{-1} \text{ s}^{-1}$). Theoretically, three investigations are on record for this reaction. In 1975, Choo et al. studied this reaction using the bond-energy bond-order (BEBO) method of Johnston,¹³ and found that the activation energy was overestimated with respect to the experimental data. In 1999, Espinosa-Garcia¹⁴ constructed the potential energy surface of this reaction. Thermal and vibrational state selected rate constants were obtained over the temperature range of 200–500 K. In 2000, Yu et al.¹⁵ studied the reaction using ab initio molecular orbital theory combined with the canonical variational transition state theory (CVT).^{16–18} The geometric parameters and frequencies were obtained at the QCISD/

6-311+G(d,p) level, and the energies were calculated at the G2 theory. The rate constants were deduced over a temperature range of 200–1600 K, and a three-parameter expression was fitted: $k = 2.0 \times 10^7 T^{2.12} \exp(-492)/T$ (in $\text{cm}^3 \text{ molecule}^{-1} \text{ s}^{-1}$). It can be seen that the reaction of H with GeH_4 has ever been investigated theoretically by Espinosa-Garcia and Yu et al. at much higher levels. We studied this reaction for two purposes: (1) for comparison with the reactions of H with chlorogermanes; (2) for testing the reliability of our calculations. It is well-known that there is a significant computational difficulty in treating relatively large electronic systems containing several heavier atoms. Although the theory level of QCISD/6-311+G(d,p) gives better values of the geometric parameters, they are too computationally intensive to be generally applicable for the reactions of H with chlorogermanes, especially for the reaction of H with GeHCl_3 (it needs a greater computational condition). In this paper, we have used the reliable experimental and theoretical data of the reaction of H with GeH_4 to make a serious test of the applicability of the current quantum chemistry methodologies. The idea is to find a viable theory level that should be inexpensive but adequate for the reactions of H with chlorogermanes.

However, for the reactions of H with GeH_3Cl , GeH_2Cl_2 , and GeHCl_3 , the situation has been poorer still. To the best of our knowledge, no experimental or theoretical attention has been paid to these reactions.

Here we present the first systematic and theoretical study on the reactions of atomic H with chlorogermanes. First, we have examined the reaction mechanisms at high levels of ab initio molecular orbital theory. In a second step, we have carried out the kinetics calculation for the four title reactions. Our theoretical results might be useful not only for further experimental measurements in the kinetics communities but also for computer-modeling studies directed toward obtaining an understanding of the factors controlling CVD processes.

* Corresponding author. E-mail: guojz@icm.sdu.edu.cn.

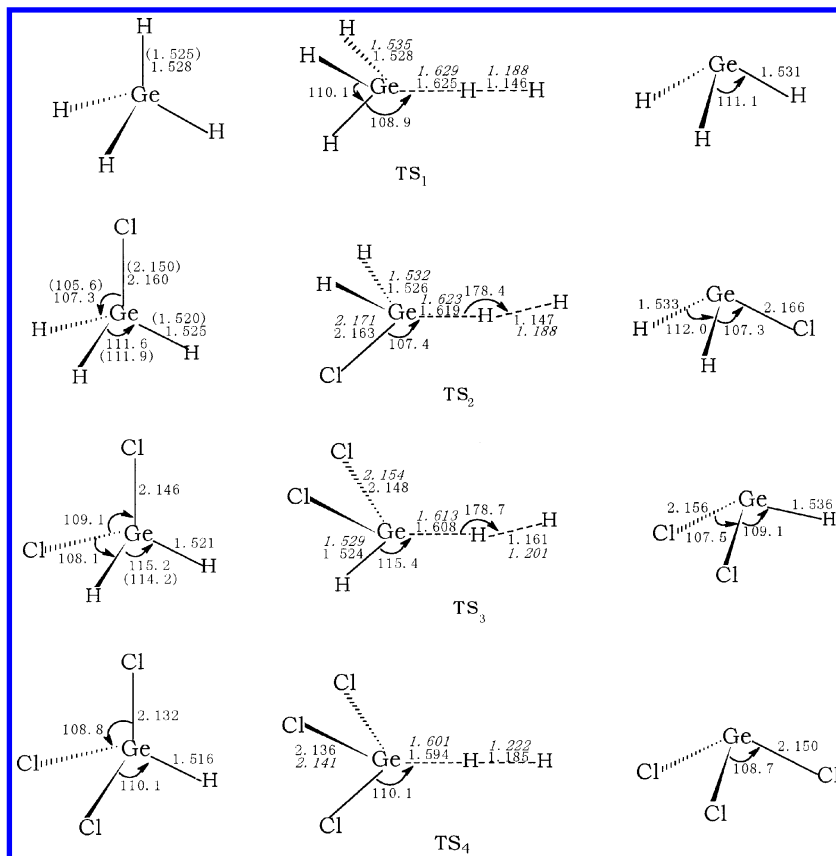


Figure 1. Optimized geometries for reactants, transition states, and products at the MP2/6-31G(d,p) level. The values in parenthesis are the experimental data.^{22–23} The values in italics are calculated at the MP2/6-311G(2d,2p) level. The bond lengths are in angstroms and the bond angles are in degrees.

2. Computation Method and Theory

Ab initio calculations have been carried out using Gaussian 94 and 98 programs.¹⁹ In the whole paper, MP2 and QCISD(T) denote the unrestricted versions, UMP2 and UQCISD(T). The geometries of the reactants, transition states, and products have been optimized at the second-order Moller–Plesset level of theory, including all the electrons in correlation calculations (MP2 = full), using the standard 6-31G(d,p) basis set for all the reactions. The vibrational frequencies (scaled by a factor of 0.95) have been calculated at the same level of theory in order to determine the nature of the stationary points, the zero-point energy (ZPE), and the thermal contributions to the free energy of activation. The intrinsic reaction coordinate (IRC) calculation confirms that the transition state connects the designated reactants and products. At the MP2/6-31G(d,p) level, the minimum energy path (MEP) has been obtained with a gradient step size of 0.02 amu^{1/2} bohr in mass-weighted Cartesian coordinates for each reaction. The force constant matrices of the stationary points and selected nonstationary points near the transition state along the MEP have also been calculated for all the reactions. To obtain accurate energies for the subsequent kinetics calculation, the single-point energies have been calculated at MP2 and QCISD(T) levels for the reaction of H with GeH_4 . The largest basis set used in the above energy calculations is 6-311+G(3df,2p). The QCISD(T)/6-311+G(3df,2p) level has been used for the reactions of H with chlorogermanes.

The initial information obtained from our ab initio calculations allowed us to calculate the variational rate constant including the tunneling effect. The canonical variational theory (CVT)^{16–18} rate constant for temperature T is given by

$$k^{\text{CVT}}(T) = \min_s k^{\text{GT}}(T, s) \quad (1)$$

where

$$k^{\text{GT}}(T, s) = \frac{\sigma k_B T}{h} \frac{Q^{\text{GT}}(T, s)}{\Phi^{\text{R}}(T)} \exp[-V_{\text{MEP}}(s)/k_B T] \quad (2)$$

where $k^{\text{GT}}(T, s)$ is the generalized transition state theory rate constant at the dividing surface s , σ is the symmetry factor accounting for the possibility of more than one symmetry-related reaction path, k_B is Boltzmann's constant, h is Planck's constant, $\Phi^{\text{R}}(T)$ is the reactant partition function per unit volume, excluding symmetry numbers for rotation, and $Q^{\text{GT}}(T, s)$ is the partition function of a generalized transition state at s with a local zero of energy at $V_{\text{MEP}}(s)$ and with all rotational symmetry numbers set to unity. All the kinetics calculations have been carried out using the POLYRATE 7.8 program.²⁰ The rotational partition functions were calculated classically, and the vibrational modes were treated as quantum-mechanical separable harmonic oscillators. Finally, we considered the tunneling effect correction. Since the heavy–light–heavy mass combination is not present in these hydrogen abstraction reactions, the tunneling correction is calculated using the centrifugal-dominant small curvature tunneling approximation (SCT).²¹

3. Results and Discussion

The optimized geometries of reactants, transition states, and products are shown in Figure 1. The vibrational frequencies of reactants, products, and transition states are listed in Tables 1 and 2. The calculated classical potential barriers ΔE and the

TABLE 1: Calculated Frequencies (in cm^{-1}) and Zero-Point Energies (ZPE, in kcal/mol) for Reactants and Products Involved in the Reactions of H with $\text{GeH}_{(4-n)}\text{Cl}_n$ ($n = 0, 1, 2, 3$) at the MP2/6-31G(d,p) Level^a

species	frequencies									ZPE
GeH_4	2223	2223	2223	2215	908	908	808	808	808	18.77
	2114	2114	2114	2106	913	913	819	819	819	
GeH_3Cl	2241	2241	2232	858	858	835	584	584	404	15.50
	2128	2128	2120	873	873	847	602	602	423	
GeH_2Cl_2	2261	2251	835	769	641	500	421	404	143	11.46
	2150	2135	854	779		524	435	410		
GeHCl_3	2269	692	692	430	430	396	171	138	138	7.66
	2156	708	708	454	454	418	181	145	145	
GeH_3	2212	2212	2185	846	846	689				12.85
GeH_2Cl	2200	2167	823	657	583	400				9.77
GeHCl_2	2150	662	577	410	391	137				6.19
GeCl_3	411	411	372	163	130	130				2.31

^a The values in italics are experimental data.^{23–26}**TABLE 2: Calculated Frequencies (in cm^{-1}) and Zero-Point Energies (ZPE, in kcal/mol) for Transition States Involved in the Reactions of H with $\text{GeH}_{(4-n)}\text{Cl}_n$ ($n = 0, 1, 2, 3$) at the MP2/6-31G(d,p) Level**

species	frequencies									ZPE
TS_1	2224	2224	2207	1192	988	988	851	851	774	18.55
	338	338	1454i							
TS_2	2233	2216	1210	981	963	841	672	598	402	15.18
	314	188	1454i							
TS_3	2230	1248	956	937	683	590	418	398	191	11.41
	187	141	1431i							
TS_4	1309	902	902	425	425	388	188	188	167	7.38
	135	135	1372i							

TABLE 3: Calculated Classical Potential Barriers ΔE and Reaction Enthalpies ΔH for the Reaction of H with GeH_4 at Various Theory Levels

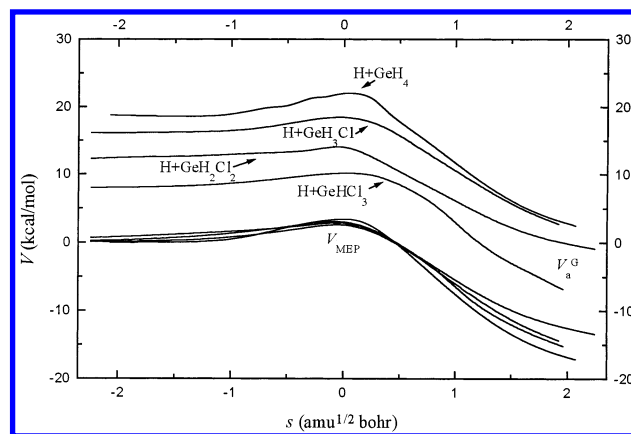
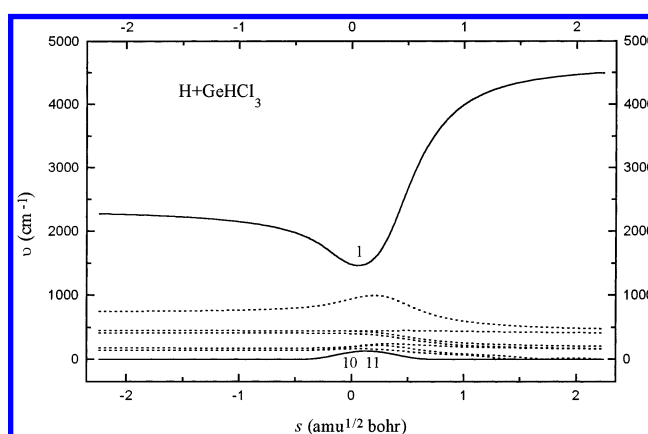
theory level	ΔE	ΔH
MP2/6-31G(d,p)	8.28	−16.01
MP2/6-311gG(2d,2p)	6.37	−18.01
MP2/6-311+G(3df,2p)	6.29	−17.93
MP2/6-311+G(3df,2p)	5.74	−18.01
QCISD(T)/6-311G(d,p)	4.71	−19.75
QCISD(T)/6-311+G(3df,2p)	3.49	−20.03
G2//QCISD/6-311+G(d,p)	3.54 ^a	−19.22 ^a
	2.53 ^b	−21.41 ^b
expt		−21.21

^a The values were done at G2//QCISD/6-311+G(d,p) by Yu.¹⁵ ^b The values were obtained from the potential energy surface.¹⁴**TABLE 4: Calculated Classical Potential Barriers ΔE (in kcal/mol), Reaction Enthalpies ΔH (in kcal/mol), and the Ge–H Bond Dissociation Energies $D_0(\text{GeH}_{(3-n)}\text{Cl}_n-\text{H})$ ($n = 0, 1, 2, 3$) for the Hydrogen Abstraction Reactions of H with Germane and Chlorogermanes at the QCISD(T)/6-311+G(3df,2p)//MP2/6-31G(d,p) Level^a**

reactions	ΔE	ΔH	$D_0(\text{Ge}-\text{H})$
$\text{H} + \text{GeH}_4$	3.49	−20.03	81.23
$\text{H} + \text{GeH}_3\text{Cl}$	3.44	−20.73	80.71
	14.46	−6.05	
$\text{H} + \text{GeH}_2\text{Cl}_2$	3.20	−22.10	79.50
	14.74	−5.90	
$\text{H} + \text{GeHCl}_3$	2.86	−23.54	78.28
	14.00	−7.67	

^a The values in italics are the potential barrier and the enthalpies of the chlorine abstraction.

reaction enthalpies ΔH are summarized in Table 3 for the reaction of H with GeH_4 and in Table 4 for the reactions of H with chlorogermanes. Figure 2 depicts the change curves of the classical potential energy (V_{MEP}) and vibrationally adiabatic

**Figure 2.** Classical potential energy (V_{MEP}) and the vibrationally adiabatic potential energy (V_a^G) curves as functions of s for the reactions of H with $\text{GeH}_{(4-n)}\text{Cl}_n$ ($n = 0, 1, 2, 3$) at the QCISD(T)/6-311+g(3df,2p)//MP2/6-31G(d,p) level.**Figure 3.** Changes of the generalized normal-mode vibrational frequencies as functions of s at the MP2/6-31(d,p) level for the reaction of H with GeHCl_3 .

potential energy (V_a^G) curves with the reaction coordinate s at the QCISD(T)/6-311+G(3df,2p)//MP2/6-31G(d,p) level for all the reactions. Change curves of the generalized normal-mode vibrational frequencies with the reaction coordinate s are shown in Figure 3 for the reaction of H with GeHCl_3 . The calculated TST, CVT, and CVT/SCT rate constants along with the experimental values are presented in Figure 4.

3.1. Reaction Mechanism. As mentioned above, the reactions of H with GeH_3Cl , GeH_2Cl_2 , and GeHCl_3 can proceed via two channels: hydrogen abstraction from the Ge–H bonds and chlorine abstraction from the Ge–Cl bonds. The barrier heights calculated at the QCISD(T)/6-311+G(3df,2p) level are 3.44, 3.20, and 2.86 kcal/mol for hydrogen abstraction from GeH_3Cl , GeH_2Cl_2 , and GeHCl_3 , while the barrier heights of chlorine abstraction are 14.46, 14.74, and 14.00 kcal/mol, respectively. The latter are much higher than the former. Thus, we can safely say that chlorine abstraction is negligible for the reactions of H with GeH_3Cl , GeH_2Cl_2 , and GeHCl_3 , which is very similar to the mechanism of the reactions of H with SiH_3Cl , SiH_2Cl_2 , and SiHCl_3 .⁶ Therefore, we mainly discuss hydrogen abstraction from GeH_3Cl , GeH_2Cl_2 , and GeHCl_3 in the following study.

a. Geometry and Frequency. It is worth stating the reliability of the calculations in this work. Since unrestricted Hartree–Fock (UHF) reference wave functions are not spin eigenfunctions for open-shell species, we monitored the expectation values of $\langle S^2 \rangle$ in the MP2 optimization.²⁷ The values of $\langle S^2 \rangle$ are always in the range of 0.750–0.772 for doublets at the MP2/6-31G(d,p) level. After spin annihilation, the values of $\langle S^2 \rangle$ are 0.750, where

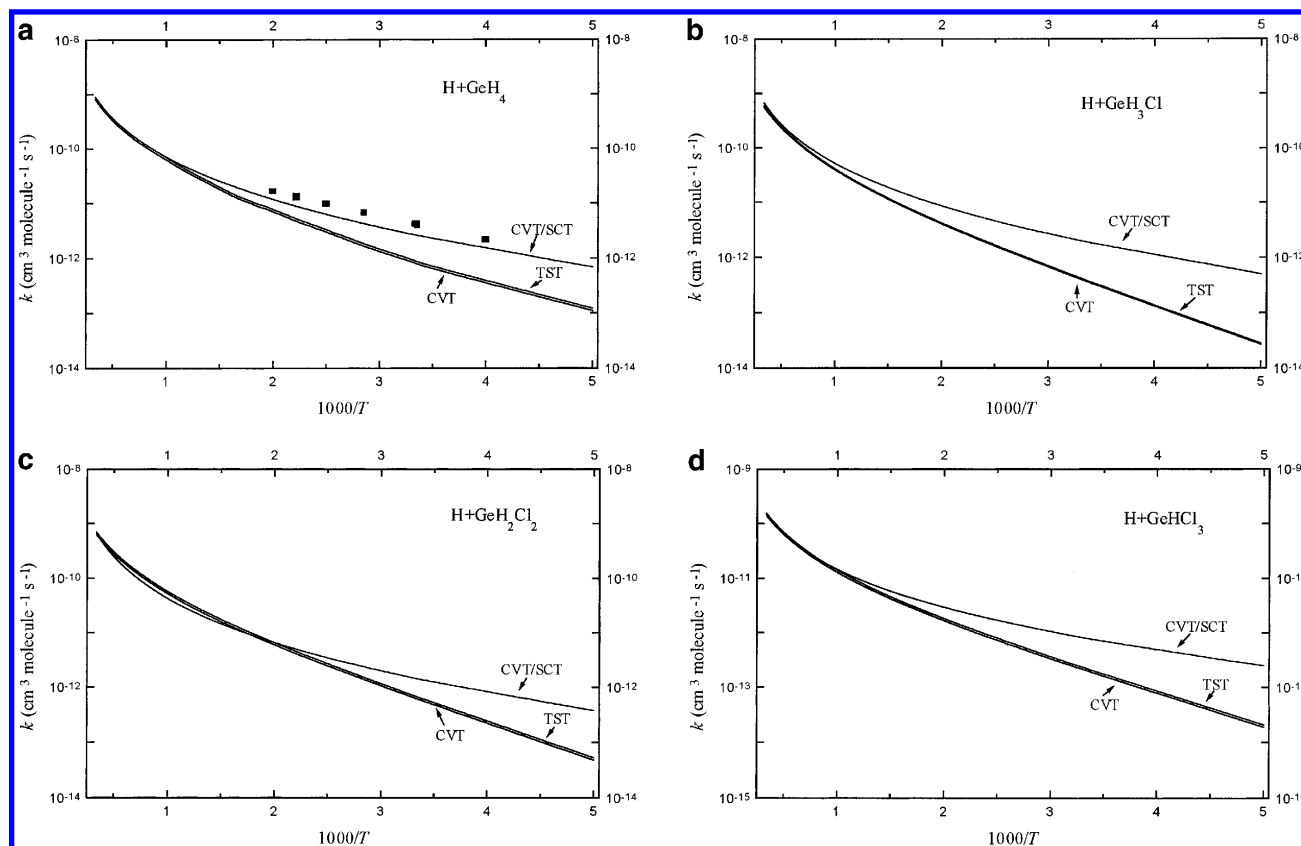


Figure 4. (a–d) Rate constant as a function of the reciprocal of the temperature (K) over the temperature range of 200–3000 K for the reactions of H with $\text{GeH}_{(4-n)}\text{Cl}_n$ ($n = 0, 1, 2, 3$). ■ are the experimental values.

0.750 is the exact value for a pure doublet. Thus, spin contamination is not severe in the MP2/6-31G(d,p) optimization for all the title reactions. This suggests that a single determinant reference wave function is suitable for the level of theory used in the optimization.

To clarify the general reliability of the theoretical calculations, it is useful to compare the predicated chemical properties of the present particular systems of interest with experimental data. As shown in Figure 1, the maximum error of the calculated geometric parameters of GeH_4 , GeH_3Cl , and GeH_2Cl_2 are less than 0.5% compared with the experimental values. From this result, it might be inferred that the same accuracy could be expected for the calculated transition state geometries, but such an inference would be unjustified because transition states are much harder to calculate. To check the dependence of the ab initio results on the basis set, we performed the MP2 calculation with the flexible 6-311G(2d,2p) (computationally more expensive) for the transition states. The optimized geometrical parameters are also shown in Figure 1. Comparison shows that the extension of basis set, 6-311G(2d,2p), does not cause observable change. As can be seen from Table 1, the vibrational frequencies of GeH_4 , GeH_3Cl , GeH_2Cl_2 , and GeHCl_3 agree well with the experimentally observed fundamentals, and the maximum relative error is less than 5.5%. These good agreements give us confidence that the MP2/6-31G(d,p) theory level is adequate to optimize the geometries and calculate the frequencies.

The transition states of hydrogen abstraction from GeH_4 , GeH_3Cl , GeH_2Cl_2 , and GeHCl_3 are denoted as TS_1 , TS_2 , TS_3 , and TS_4 , respectively. Their geometrical parameters calculated at the MP2/6-31G(d,p) level are shown in Figure 1. For the reactions of H with GeH_4 and GeHCl_3 , the H atom attacks linearly the H of the Ge–H bond, and the transition states TS_1

and TS_4 have C_{3v} symmetry. For the reactions of H with GeH_3Cl and GeH_2Cl_2 , the H atom attacks one H of the Ge–H bonds with a slightly bent orientation angle of 178.4° and 178.7° , respectively. Thus, the transition states TS_2 and TS_3 have C_s symmetry. For the transition states TS_1 , TS_2 , TS_3 , and TS_4 , the breaking Ge–H bonds are elongated by 6.35%, 6.16%, 5.72%, and 5.15%, while the forming H–H bonds are longer than the equilibrium value of 0.734 \AA in H_2 by 56.13%, 56.27%, 58.17%, and 61.44%, respectively. Therefore, TS_1 , TS_2 , TS_3 , and TS_4 are reactant-like, and the hydrogen abstraction reactions from germane and chlorogermanes proceed via early transition states. This rather early character in these transition states is in accordance with the low reaction barrier and the high exothermicity of these reactions, in keeping with Hammond's postulate.²⁸ In addition, from GeH_4 to GeHCl_3 , the transition state via which the reaction will proceed occurs earlier and earlier.

Table 2 shows that transition states of hydrogen abstraction from GeH_4 , GeH_3Cl , GeH_2Cl_2 , and GeHCl_3 have one and only one imaginary frequencies. Since the imaginary frequency governs the width of the classical potential energy barrier along the MEP, it plays an important role in the tunneling calculations, especially when the imaginary frequency is large, and the associated eigenvector has a large component of hydrogenic motion. For the four title reactions, the values of the imaginary frequencies are large, which implies that the quantum tunneling effect may be significant and may play an important role in the calculation of the rate constant.

b. Energy. To choose a reliable theory level to calculate the energy, we calculated potential barriers ΔE and reaction enthalpies ΔH at various levels of theory for the reaction of H with GeH_4 . The values are listed in Table 3. First, we analyze the reaction enthalpy. Espinosa-Garcia¹⁴ obtained a better experimental value of -21.21 kcal/mol from the measured $\Delta H_{f,0}$

for GeH_4 , GeH_3 , and H. The values calculated at the MP2 level with different basis sets are in great disagreement with this experimental value; a similar calculation with the highly correlated and more computationally demanding QCISD(T) level predicts the value that is in excellent agreement with the experimental result, especially if the experimental uncertainty for GeH_3 (± 2 kcal/mol) is taken into consideration. This result clearly indicated that most of the error in the reaction enthalpy computed at the MP2 level can be attributed to lack of correlation in the method and not to an improper optimized geometry at the MP2/6-31G(d,p) level.

With respect to the barrier height, a direct comparison of theory with experiment is not possible. It can be seen from Table 3 that the potential barriers have a great discrepancy obtained at different levels for the reaction of H with GeH_4 . The values calculated at the MP2 level with different basis sets are greater than those obtained at the QCISD(T) level. The value calculated at QCISD(T) level with 6-311G(d,p) basis set is greater by about 0.7 kcal/mol than that calculated at the same level with 6-311+G(3df,2p) basis set. This means that the size of the basis set will have an important effect on the calculation of the potential barrier. Taking into account the calculated results of the reaction enthalpies at these levels, we think the QCISD(T)/6-311+G(3df,2p) level is the most reliable level. Therefore, in this work, we have chosen the QCISD(T)/6-311+G(3df,2p) level to calculate the potential barriers and the reaction enthalpies for the reactions of H with chlorogermanes.

It is worth discussing the effect of chlorine substitution on the reaction mechanism for the reactions of H with GeH_4 , GeH_3Cl , GeH_2Cl_2 , and GeHCl_3 . There are three features for the four reactions. First, the potential barrier of the reaction of H with GeH_4 is 3.49 kcal/mol at the QCISD(T)/6-311+G(3df,2p) level, while the potential barriers of the reactions of H with GeH_3Cl , GeH_2Cl_2 , and GeHCl_3 are 3.44, 3.20, and 2.86 kcal/mol, respectively. There is a very slight decrease in barrier height along the series from GeH_4 to GeHCl_3 . The barrier heights of the reactions of H with GeH_4 and GeH_3Cl are nearly identical. The potential barrier of the reaction of H with GeHCl_3 is 0.63 kcal/mol lower than that of the H with GeH_4 reaction. Second, the reaction enthalpy of the reaction of H with GeH_4 is -20.03 kcal/mol at the QCISD(T)/6-311+G(3df,2p) level, while the values are -20.73 , -22.10 , and -23.54 kcal/mol for the reactions of H with GeH_3Cl , GeH_2Cl_2 , and GeHCl_3 . The exothermicities of the reactions of H with chlorogermanes are greater than that of H with GeH_4 , and the exothermicity increases with the increase in chlorine substitution from GeH_3Cl to GeHCl_3 through GeH_2Cl_2 . Third, the dissociation energy of the Ge–H bond in GeH_4 is 81.23 kcal/mol at the QCISD(T)/6-311+G(3df,2p) level, while the Ge–H bond dissociation energies in GeH_3Cl , GeH_2Cl_2 , and GeHCl_3 are 80.71, 79.50, and 78.28 kcal/mol, respectively. There is a slight decrease in Ge–H bond dissociation energies along the series from GeH_4 to GeHCl_3 . The above analysis suggests that chlorine substitution has only a slight effect on the reactivity and the strength of the Ge–H bond. The following kinetics study further testifies to this view.

3.2. Kinetics Calculations. *a. Reaction Path Properties.* With a step size of $0.05 \text{ amu}^{1/2} \text{ bohr}$, the intrinsic reaction coordinate (IRC) has been calculated at the MP2/6-31G(d,p) level from the transition state to the reactants and the products for each reaction. For the reaction of H with GeH_3Cl , the breaking Ge–H bond is almost unchanged from $s = -\infty$ to $s = -0.5 \text{ amu}^{1/2} \text{ bohr}$ and equals the value in the reactant, and stretches linearly after $s = -0.5 \text{ amu}^{1/2} \text{ bohr}$. The forming H–H bond shortens

rapidly from reactants and reaches the equilibrium bond length in H_2 at $s = 0.5 \text{ amu}^{1/2} \text{ bohr}$. Other bond lengths are almost unchanged during the reaction process. Therefore, the transition state TS_2 connects the reactants (GeH_3Cl and H) with the products (GeH_2Cl and H_2). The geometric change mainly takes place in the region from $s = -0.5$ to $s = 0.5 \text{ amu}^{1/2} \text{ bohr}$. This means that the region of the hydrogen abstraction reaction path represents the main interaction of the reaction process. The same conclusion can be drawn from the reactions of H with GeH_4 , GeH_2Cl_2 , and GeHCl_3 .

The minimum energy path (MEP) was calculated at the MP2/6-31G(d,p) level by the IRC definition with a step size of $0.02 \text{ amu}^{1/2} \text{ bohr}$. The potential energy profile was further improved at the QCISD(T)//MP2 level. For all the reactions the maximum position of the classical potential energy curve V_{MEP} at the QCISD(T)//MP2 level corresponds to the saddle point structure at the MP2/6-31G(d,p) level. Therefore, the shifting of the maximum position for the V_{MEP} curve caused by the computational technique is avoided.²⁹ The changes of the classical potential energy V_{MEP} and the ground state vibrational adiabatic potential energy V_a^{G} with the reaction coordinate s are shown in Figure 2 for the reactions of H with GeH_4 , GeH_3Cl , GeH_2Cl_2 , and GeHCl_3 . It is interesting to note that the change trend of V_{MEP} and V_a^{G} are similar for these four reactions: this means that they have a similar reaction mechanism. It can be also seen from Figure 2 that the maximum positions of V_{MEP} and V_a^{G} energy curves are almost the same at the QCISD(T)//MP2 level for each reaction. The zero-point energy ZPE, which is the difference of V_a^{G} and V_{MEP} , is almost unchanged as s varies. This means the variational effect will be small for the four reactions. To analyze this behavior in greater detail, we show the variation of the generalized normal-mode vibrational frequencies as functions of s in Figure 3 for the reaction of H with GeHCl_3 .

Along the MEP a generalized normal-mode analysis has been performed using rectilinear Cartesian coordinates for each reaction. In the negative limit of s , the frequencies are associated with the reactants, while in the positive limit of s , the frequencies are associated with the products. For the sake of clarity, the vibrational frequencies can be divided into three types: spectator modes, transitional modes, and reactive modes. The spectator modes are those that undergo little change and sometimes remain basically unchanged in going from reactants to the transition state. The transitional modes appear along the reaction path as a consequence of the transformation from free rotation or free translations within the reactant or the product limit into real vibrational motions in the global system. Their frequencies tend to zero at the reactant and the product limit and reach their maximum in the saddle point zone. The reactive modes are those that undergo the largest change in the saddle point zone, and therefore, they must be related to the breaking/forming bonds. For the reaction of H with GeHCl_3 , the mode 1 that connects the frequency of Ge–H stretching vibration of reactant with the frequency of the H–H stretching vibration of H_2 is the reactive mode. Modes 10 and 11 are transitional modes, and other modes are spectator modes. From $s = -1.0$ to $s = 1.0 \text{ amu}^{1/2} \text{ bohr}$, the reactive mode drops dramatically; this behavior is similar to that found in other hydrogen abstraction reactions.^{30–32} A priori, this drop should cause a considerable fall in the zero-point energy curve near the transition state. However, this kind of drop of the reactive mode is compensated by the transitional modes. As a result, the zero-point energy shows very little change during the reaction process and the classical potential energy V_{MEP} and the ground state vibrational adiabatic

potential energy V_a^G curves are similar in shape. For the same reason, the V_{MEP} and V_a^G curves are similar in shape for the reactions of H with GeH_4 , GeH_3Cl , and GeH_2Cl_2 .

b. Rate Constants. Canonical variational transition state theory (CVT) with small curvature tunneling correction (SCT), which has been successfully performed for several analogous reactions,^{5–8} is an effective method to calculate the rate constants. In this paper, we used this method to study the kinetic properties for the reactions of H with GeH_4 , GeH_3Cl , GeH_2Cl_2 , and GeHCl_3 over a wide temperature range from 200 to 3000 K.

To calculate the rate constants, 30 points are selected near the transition state along the MEP for each reaction, 15 points on the reactant side and 15 points on the product side. The calculated CVT/SCT rate constants along with the experimental values are shown in Figure 4 for these four reactions. The calculated transition state theory (TST) and CVT values are also depicted in Figure 4 for comparison purposes. Several important features of the calculated rate constants are the following:

1. For the four reactions, the TST and CVT rate constants are almost the same over the whole studied temperature range, which enables us to conclude that the variational effect is small for the calculation of the rate constant.

2. Reactions involving hydrogen atom transfer are usually characterized by a significant tunneling effect that must be accounted for when computing reaction rate constants. For all the reactions, in the lower temperature ranges the CVT rate constants are smaller than those of CVT/SCT. With the increase in temperature, the CVT/SCT rate constants are asymptotic to those of TST and CVT. This means only in the lower temperature ranges does the small curvature tunneling correction play an important role for these reactions.

3. For the reaction of GeH_4 and H, the calculated CVT/SCT rate constants are in excellent agreement with the experimental values over the temperature range of 293–473 K. Therefore, the CVT/SCT method is a good choice to calculate accurate rate constants for the title systems. Both the TST method and the CVT method without the tunneling effect correction underestimate rate constants. Because the reactions of H with germane and chlorogermanes have similar reaction mechanisms, the CVT/SCT rate constants for the reactions of H with chlorogermanes (namely GeH_3Cl , GeH_2Cl_2 , and GeHCl_3) are expected to have similar accuracy.

4. It is obvious that the calculated rate constants exhibit typical non-Arrhenius behavior. This non-Arrhenius behavior has frequently been observed in radical–molecule reactions studied over wide temperature ranges. The CVT/SCT rate constants of the title reactions are fitted by three-parameter formulas over the temperature range of 200–3000 K and given in units of $\text{cm}^3 \text{ molecule}^{-1} \text{ s}^{-1}$ as follows:

$$k_1 = 3.09 \times 10^{-17} T^{2.16} \exp(-286.74/T) \text{ for H with } \text{GeH}_4$$

$$k_2 = 1.94 \times 10^{-17} T^{2.18} \exp(-276.82/T) \text{ for H with } \text{GeH}_3\text{Cl}$$

$$k_3 = 4.19 \times 10^{-18} T^{2.37} \exp(-227.64/T) \text{ for H with } \text{GeH}_2\text{Cl}_2$$

$$k_4 = 2.02 \times 10^{-17} T^{1.98} \exp(-218.51/T) \text{ for H with } \text{GeHCl}_3$$

5. The effect of chlorine substitution on the reactivity of the Ge–H bond can be seen by evaluating the room temperature k/n , the room temperature rate constant corrected for the reaction path degeneracy, and where n is the number of the Ge–H bonds. At 298 K, k/n for the reaction of H with GeH_4 is $6.52 \times 10^{-13} \text{ cm}^3 \text{ molecule}^{-1} \text{ s}^{-1}$; for the reactions of H with GeH_3Cl ,

GeH_2Cl_2 , and GeHCl_3 , the values of k/n are 6.37×10^{-13} , 7.05×10^{-13} , and $7.84 \times 10^{-13} \text{ cm}^3 \text{ molecule}^{-1} \text{ s}^{-1}$, respectively. The k/n values of the reactions of H with GeH_4 and GeH_3Cl are nearly identical. The k/n values of H with GeH_2Cl_2 and GeHCl_3 are slightly larger than that of H with GeH_4 . This means chlorine substitution has a slight effect on the reactivity of the Ge–H bond.

4. Conclusion

In this paper, we have studied systematically the reactions of H with GeH_4 , GeH_3Cl , GeH_2Cl_2 , and GeHCl_3 using ab initio and canonical variational transition state theory (CVT) with small curvature tunneling effect. Both the reaction mechanism and the rate constants were reported over the temperature range of 200–3000 K. Several major conclusions can be drawn from this calculation.

1. The four title reactions have a similar reaction mechanism. The transition states involved in these reactions have rather early character.

2. For the reactions of H with chlorogermanes, hydrogen abstraction from the Ge–H bonds is the sole channel.

3. The calculated CVT/SCT rate constants exhibit typical non-Arrhenius behavior.

4. Chlorine substitution has a slight effect on the strength and the reactivity of the Ge–H bonds in $\text{GeH}_{4-n}\text{Cl}_n$ ($n = 1–3$).

Acknowledgment. The authors thank Professor Donald G. Truhlar for providing the POLYRATE 7.8 program. This work is supported by the Research Fund for the Doctoral Program of Higher Education of China.

References and Notes

- (1) Doyle, J. R.; Doughty, D. A.; Gallagher, A. *J. Appl. Phys.* **1991**, 69, 4169.
- (2) Beaucarne, G.; Poortmans, J.; Caymax, M.; Nijs, J.; Mertens, R. *Mater. Res. Soc. Symp. Proc.* **1998**, 485, 89.
- (3) Koinuma, H.; Manako, T.; Natsuaki, H.; Fujioka, H.; Fueki, K. *J. Non-Cryst. Solids* **1985**, 77, 801.
- (4) Doyle, J. R.; Doughty, D. A.; Gallagher, A. *J. Appl. Phys.* **1992**, 71, 4727.
- (5) Zhang, Q.-Z.; Wang, S.-K.; Wang, C.-S.; Gu, Y.-S. *Phys. Chem. Chem. Phys.* **2001**, 3, 4280.
- (6) Zhang, Q.-Z.; Wang, S.-K.; Gu, Y.-S. *J. Phys. Chem. A* **2002**, 106, 3796.
- (7) Zhang, Q.-Z.; Zhang, D.-J.; Wang, S.-K.; Gu, Y.-S. *J. Phys. Chem. A* **2002**, 106, 122.
- (8) Zhang, Q.-Z.; Wang, S.-K.; Gu, Y.-S. *J. Phys. Chem. A* **2002**, 106, 9071.
- (9) Choo, K. Y.; Gaspar, P. P.; Wolf, A. P. *J. Phys. Chem.* **1975**, 79, 1752.
- (10) Austin, E. R.; Lampe, F. W. *J. Phys. Chem.* **1977**, 81, 1134.
- (11) Nava, D. F.; Payne, W. A.; Marston, G.; Stief, L. J. *J. Geophys. Res.* **1993**, 98, 5331.
- (12) Arthur, N. L.; Cooper, I. A. *J. Chem. Soc., Faraday Trans.* **1995**, 91, 3367.
- (13) Johnston, H. S. *Gas Phase Reaction Rate Constant*; Ronald: New York, 1965.
- (14) Espinosa-Garcia, J. *J. Chem. Phys.* **1999**, 111, 9330.
- (15) Yu, X.; Li, S.-M.; Sun, C.-C. *J. Phys. Chem. A* **2000**, 104, 9207.
- (16) Baldrige, K. K.; Gordon, M. S.; Steckler, R.; et al. *J. Phys. Chem.* **1989**, 93, 5107.
- (17) Gonzalez-Lafont, A.; Truong, T. N.; Truhlar, D. G. *J. Chem. Phys.* **1991**, 95, 8875.
- (18) Garrett, B. C.; Truhlar, D. G. *J. Phys. Chem.* **1979**, 83, 1052.
- (19) Frisch, M. J.; et al. *Gaussian 94 and 98*, Revision E.1; Gaussian: Pittsburgh, PA, 1995 and 1998.
- (20) Steckler, R.; Chuang, Y. Y.; Fast, P. L.; Corchade, J. C.; Coitino, E. L.; Hu, W. P.; Lynch, G. C.; Nguyen, K.; Jackells, C. F.; Gu, M. Z.; Rossi, I.; Clayton, S.; Melissas, V.; Garrett, B. C.; Isaacson, A. D.; Truhlar, D. G. *POLYRATE 7.8 Version*; University of Minnesota: Minneapolis, 1997.
- (21) Liu, Y.-P.; Lynch, G. C.; Truong, T. N.; Lu, D.-H.; Truhlar, D. C.; Garrett, B. C. *J. Am. Chem. Soc.* **1993**, 115, 2408.

- (22) Cradock, S.; McKean, D. C.; MacKenzie, M. W. *J. Mol. Struct.* **1981**, 74, 265.
- (23) Lide, D. R. In *CRC Handbook of Chemistry and Physics*, 79th ed.; CRC Press: New York, 1998.
- (24) Burger, H.; Eujen, R.; Cradock, S.; Henry, L.; Valentin, A. *J. Mol. Spectrosc.* **1986**, 116, 228.
- (25) Ebsworth, E. A. V.; Robiette, A. G. *Spectrochimica* **1964**, 20, 1639.
- (26) Ruoff, A.; Burger, H.; Biedermann, S.; Cichon, J. *Spectrochim. Acta* **1974**, 30A, 1647.
- (27) Liu, R.; Francisco, J. S. *J. Phys. Chem. A* **1998**, 102, 9869.
- (28) Hammond, G. S. *J. Am. Chem. Soc.* **1955**, 77, 334.
- (29) Espinosa-Garcia, J.; Corchado, J. C. *J. Phys. Chem.* **1995**, 99, 8613.
- (30) Truhlar, D. G.; Isaacson, A. D. *J. Chem. Phys.* **1982**, 77, 3516.
- (31) Espinosa-Garcia, J.; Corchado, J. C. *J. Phys. Chem.* **1996**, 100, 16561.
- (32) Corchado, J. C.; Espinosa-Garcia, J. *J. Chem. Phys.* **1997**, 106, 4013.